Electronic Supplementary Information

Nanoliter atmospheric pressure photoionization-mass spectrometry for direct bioanalysis of polycyclic aromatic hydrocarbons

Siyuan Tan[1]*, Xinchi Yin[1], Lulu Feng[2], Juduo Wang[1], Zhichao Xue[1], You Jiang[1], Xinhua Dai[1], Xiaoyun Gong[1]*, Xiang Fang[1]*

[1]Technology Innovation Center of Mass Spectrometry for State Market Regulation, Center for Advanced Measurement Science, National Institute of Metrology, Beijing 100029, People's Republic of China.

[2]Department of Chemistry, Zhejiang University, Hangzhou 310027, Zhejiang, China.

**Email: tansy@nim.ac.cn (Siyuan Tan)*

Electronic Supplementary Information

1. The sample preparation and the analysis of PAHs in complex biosamples

1.1. The preparation of standard PAHs sample

Standard stock solutions of PAHs were first prepared at a concentration of 5.0 mM in acetone, and stored at 4°C. Then, different types of PAHs solutions were further diluted by ACN with a range of concentration from 0.1 nM to 1000 μM. Other polar or low-polar compounds were all prepared with different concentrations in ACN.

1.2. Analysis of PAHs in fetal bovine serum.

Blood sample (FBS) was first centrifuged with 15000 r/min for 5 min to remove the precipitated solid impurity. Then the treated FBS was 50-folded diluted with 1 mM PBS and spiked with 80 nM benzo[a]anthracene, indeno[1,2,3-cd]pyrene and dibenzo[a,h]anthracene. The 0.5 μL blood sample was injected into the nano-tip and then analyzed by nano-ESI and nano-APPI.

1.3. Cell culture and single-cell analysis

K562 suspension cells were cultured in RPMI-1640 medium with 10% FBS and 1% penicillin-streptomycin at 37 °C and 5% CO_2 in a humidified incubator and passaged every 3 days. The concentration of K562 cells was determined by an automatic hemocytometer (Adam MC, Digital Bio, South Korean). For the analysis of PAHs spiked in single-cell samples, four milliliters of K562 cell suspension (10^7 cells/mL) were further passaged and cultured by RPMI-1640/FBS containing 5.0 μM benzo[a]anthracene for 2 weeks. Microscopic photographs have been taken to confirm that single cells are captured instead of multiple cells. As was shown in Figure S10, a single K562 cell was captured by nano-tip (internal diameter: 20 ± 1.0 μm) connected with BRE Micro-injector (Sutter Instrument Co., Novato, CA) under the negative pressure. The pressure was kept at −20 psi. The individual cell was then washed by 10 μL PBS for three times. The cell was quenched with 2 μL methanol and dried in vacuum freeze drier. The sample was finally redissovled with 0.5 μL ACN and analyzed by nano-ESI and nano-APPI.

For the quantification of PAHs spiked in cellular samples, four milliliters of K562 cell suspension (10^7 cells/mL) were further passaged and cultured by RPMI-1640/FBS containing various PAHs with different concentrations. Nine different PAHs were adopted, including fluoranthene, pyrene, benzo[a]anthracene, chrysene, benzo[k]fluoranthene, benzo[b]fluoranthene, benzo[a]fluoranthene,

indeno[1,2,3-cd] pyrene and dibenzo[a,h]anthrathracene. The concentration was ranging from 1.0 nM to 3.0 mM. After 24 h incubation, the cell samples were washed by 4 mL PBS for three times. The cell sample was then resuspensioned by 4 mL ACN containing a certain amount of benzo[a]anthracene-d_{12} to extract the PAHs in cells. After the centrifugation, the supernatant was obtained, and analyzed by nano-APPI and APCI.

Supplementary Materials

Figure S1. Schematic illustration of single-cell capture and nano-APPI analysis.

Figure S2. The structure diagram of Nano-APPI source: (A) ultraviolet lamp; (B) sample inlet; (C) dopant/helium; (D) dopant flow path; (E) helium flow path.

Figure S3. The influence of different types of auxiliary gas in nano-APPI. Benzo[a]anthracene with a concentration of 50 nM was selected as the analytical sample.

Figure S4. The effect of different ratios of toluene/anisole on the ionization efficiency of PAHs in nano-APPI.

Figure S5. The mass spectra of six different PAHs acquired by nano-ESI: (A) indeno[1,2,3-cd]pyrene, (B) dibenzo[a,h]anthracene, (C) fluoranthene, (D) benzo[a]anthracene, (E) benzo[k]fluoranthene and (F) chrysene. The concentrations of adopted PAHs were kept at 50 nM.

Figure S6. The mass spectra of six different PAHs acquired by nano-APPI in negative polarity: (A) indeno[1,2,3-cd]pyrene, (B) dibenzo[a,h]anthracene, (C) fluoranthene, (D) benzo[a]anthracene, (E) benzo[k]fluoranthene and (F) chrysene. The concentrations of adopted PAHs were kept at 50 nM.

Figure S7. Mass spectra of a mixture sample containing three polar compounds (L-histidine, L-arginine and sucrose) obtained by (A) nano-ESI and (B) nano-APPI. The concentrations of three compounds were kept at 50 nM.

Figure S8. Mass spectra of a mixture sample containing L-arginine and chrysene obtained by (A) nano-ESI and (B) nano-APPI. The concentrations of two compounds were kept at 50 nM.

Figure S9. The CID fragmentation patterns of $M^{\bullet+}$ of different PAHs in complex biosamples: (A) $[C_{22}H_{14}]^{\bullet+}$, (B) $[C_{22}H_{12}]^{\bullet+}$ and (C) $[C_{18}H_{12}]^{\bullet+}$ in fetal bovine serum, as well as (D) $[C_{18}H_{12}]^{\bullet+}$ in a single-cell sample.

Figure S10. Images of the sampling process of single K562 cells: (A) the device image of the single-cell capturing system; (B) the microscopic image depicting the successful capture of a single K562 cell; (C) the magnified image of the capture of a single cell.

Figure S11. The successful detection of endogenous metabolites in single cells based on (A) nano-APPI and (B) nano-ESI.

Figure S12. Chemical structure of detected sterols and fatty alcohol metabolites in single K562 cells.

Table S1. The detailed information of the CID fragmentation of different PAHs ions

Table S2. List of detected PAHs in fetal bovine serum and single cells

Table S3. List of detected sterol and fatty alcohol metabolites in single K562 cells

Table S4. The quantification results of PAHs obtained by APCI; Benzo[a]anthracene-d_{12} was used as internal standard (IS) at a concentration of 20 μM.

Table S5. The information of employed PAHs detected by nano-APPI

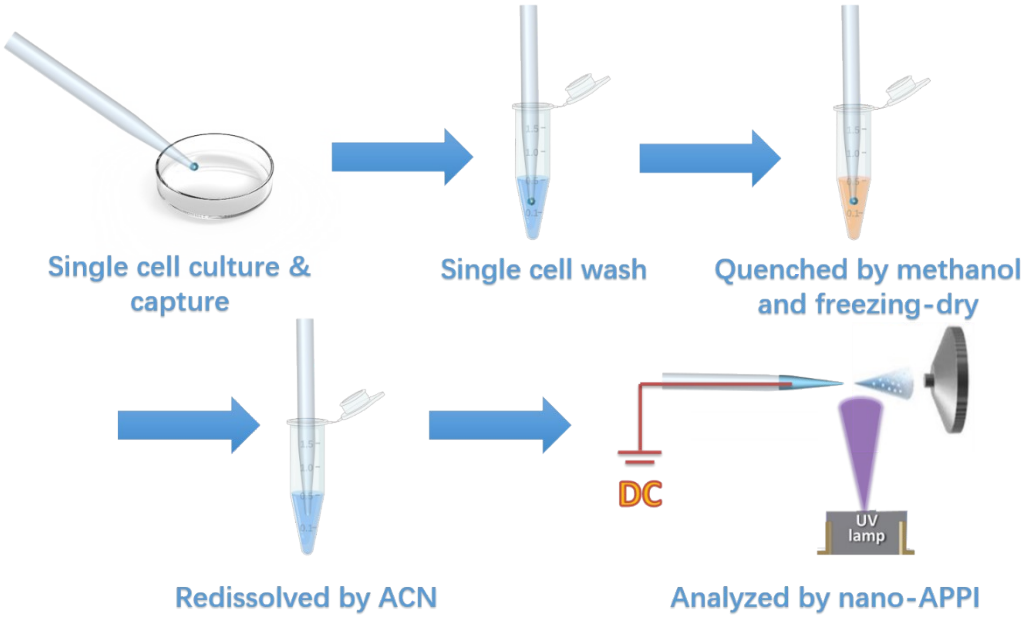

Figure S1. Schematic illustration of single-cell capture and nano-APPI analysis.

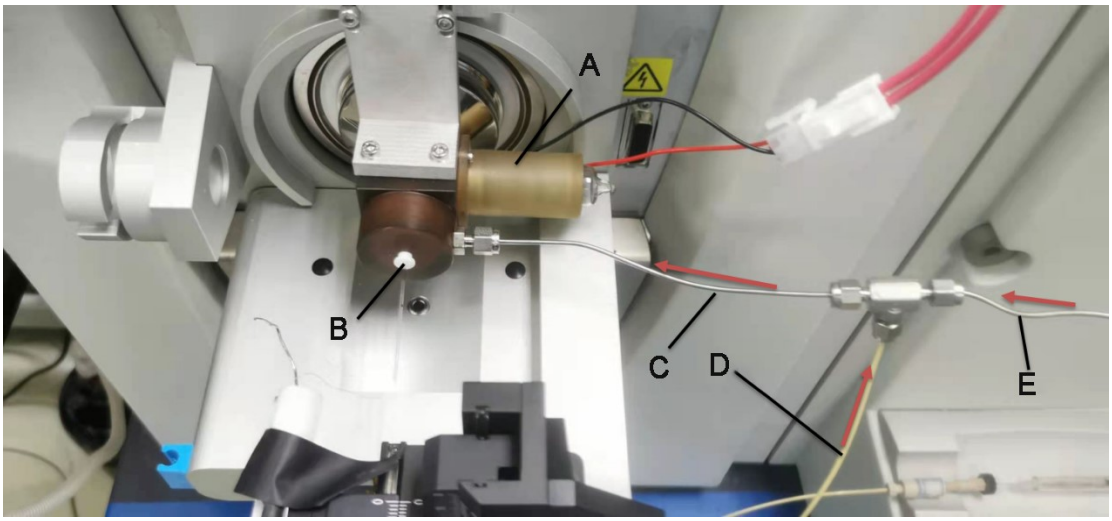

Figure S2. The structure diagram of Nano-APPI source: (A) ultraviolet lamp; (B) sample inlet; (C) dopant/helium; (D) dopant flow path; (E) helium flow path.

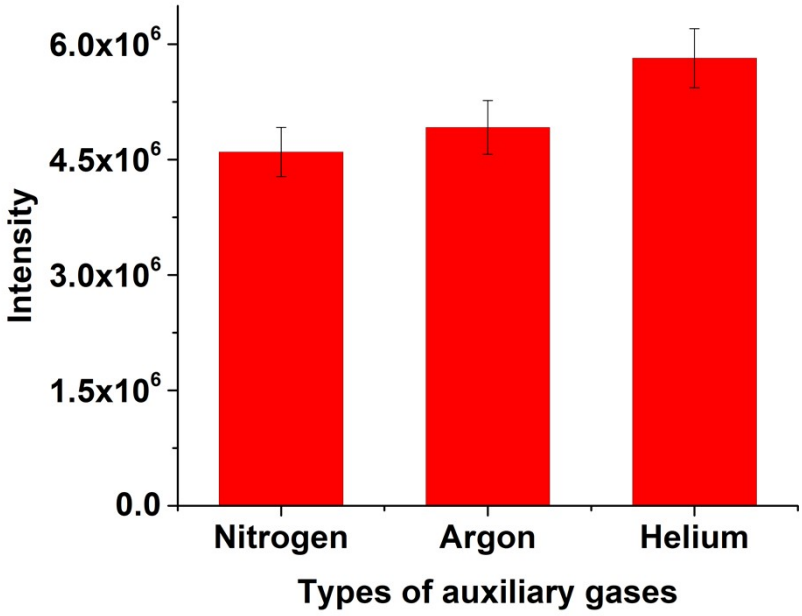

Figure S3. The influence of different types of auxiliary gas in nano-APPI. Benzo[a]anthracene with a concentration of 50 nM was selected as the analytical sample.

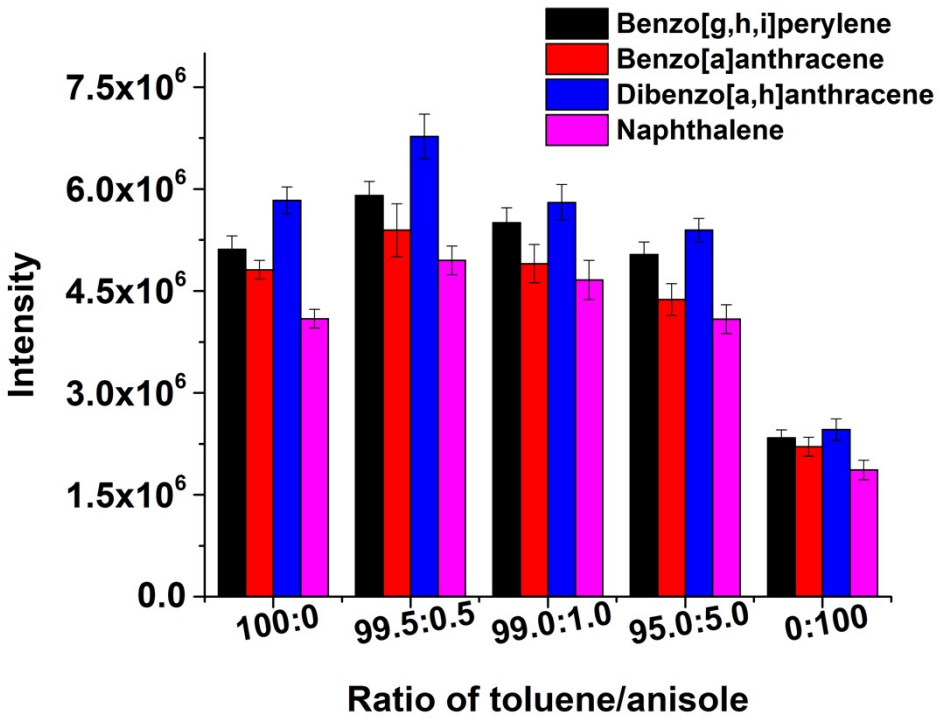

Figure S4. The effect of different ratios of toluene/anisole on the ionization efficiency of PAHs in nano-APPI.

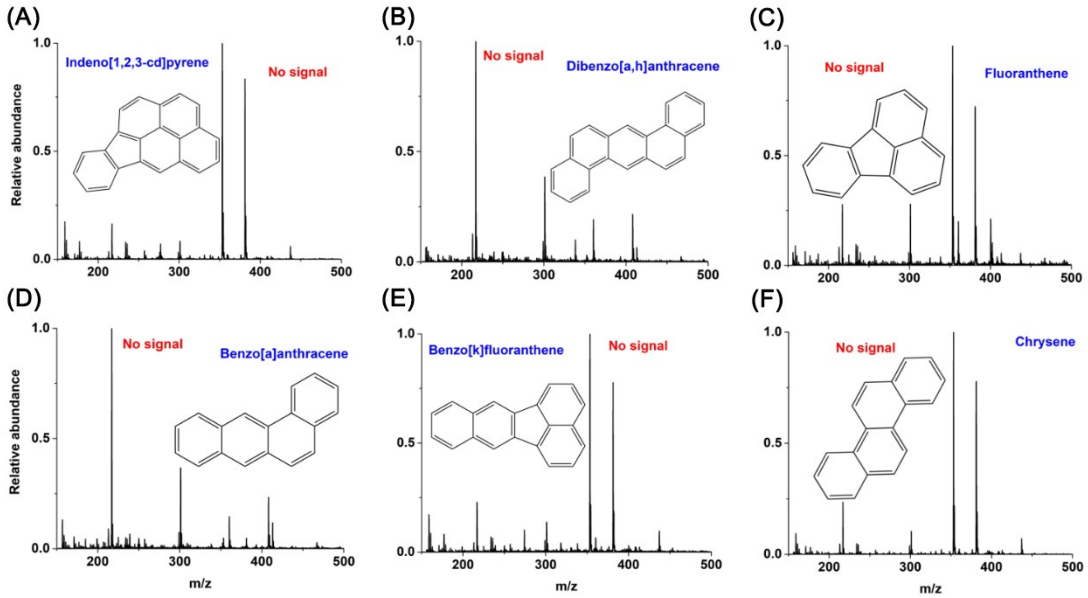

Figure S5. The mass spectra of six different PAHs acquired by nano-ESI: (A) indeno[1,2,3-cd]pyrene, (B) dibenzo[a,h]anthracene, (C) fluoranthene, (D) benzo[a]anthracene, (E) benzo[k]fluoranthene and (F) chrysene. The concentrations of adopted PAHs were kept at 50 nM.

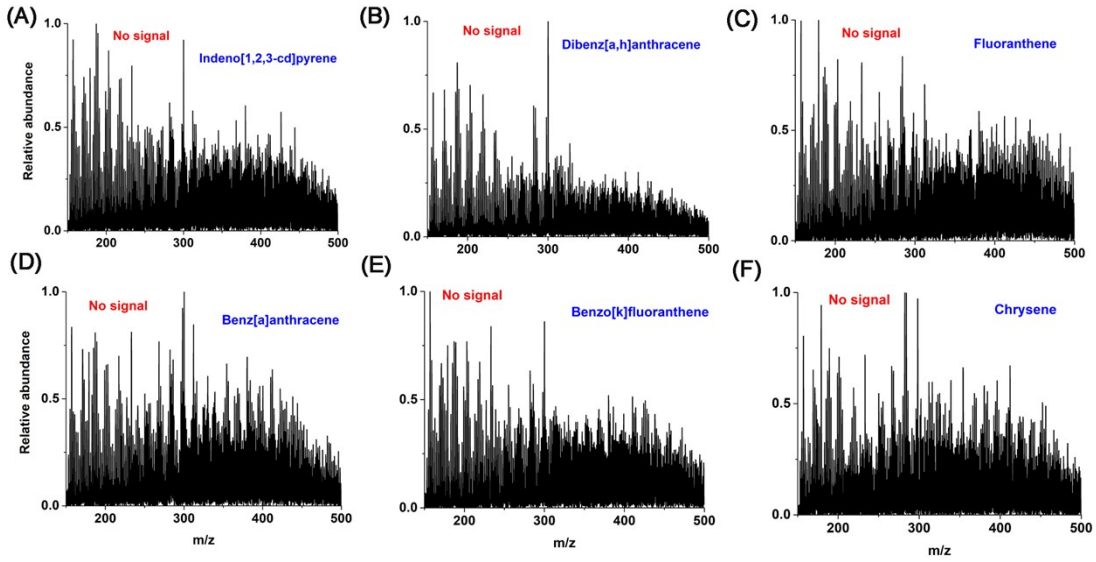

Figure S6. The mass spectra of six different PAHs acquired by nano-APPI in negative polarity: (A) indeno[1,2,3-cd]pyrene, (B) dibenzo[a,h]anthracene, (C) fluoranthene, (D) benzo[a]anthracene, (E) benzo[k]fluoranthene and (F) chrysene. The concentrations of adopted PAHs were kept at 50 nM.

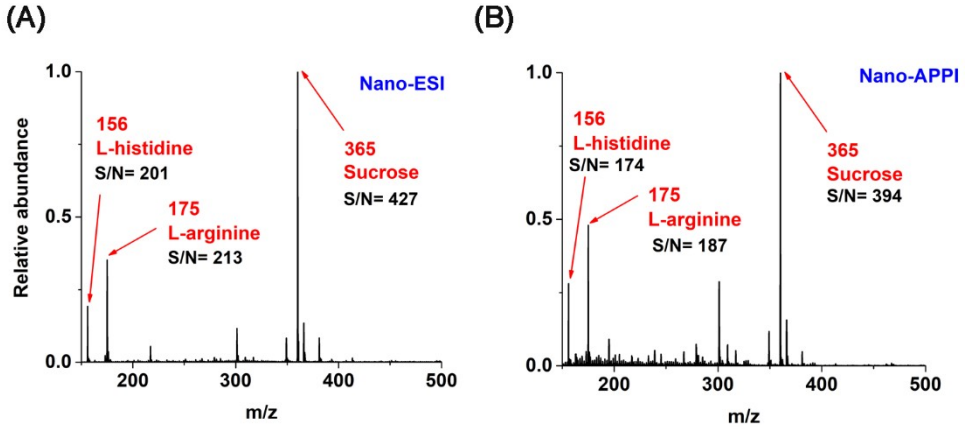

Figure S7. Mass spectra of a mixture sample containing three polar compounds (L-histidine, L-arginine and sucrose) obtained by (A) nano-ESI and (B) nano-APPI. The concentrations of three compounds were kept at 50 nM.

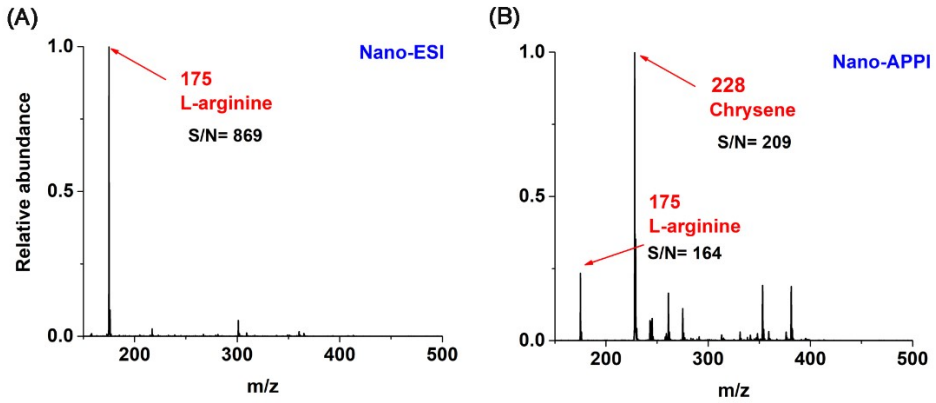

Figure S8. Mass spectra of a mixture sample containing L-arginine and chrysene obtained by (A) nano-ESI and (B) nano-APPI. The concentrations of two compounds were kept at 50 nM.

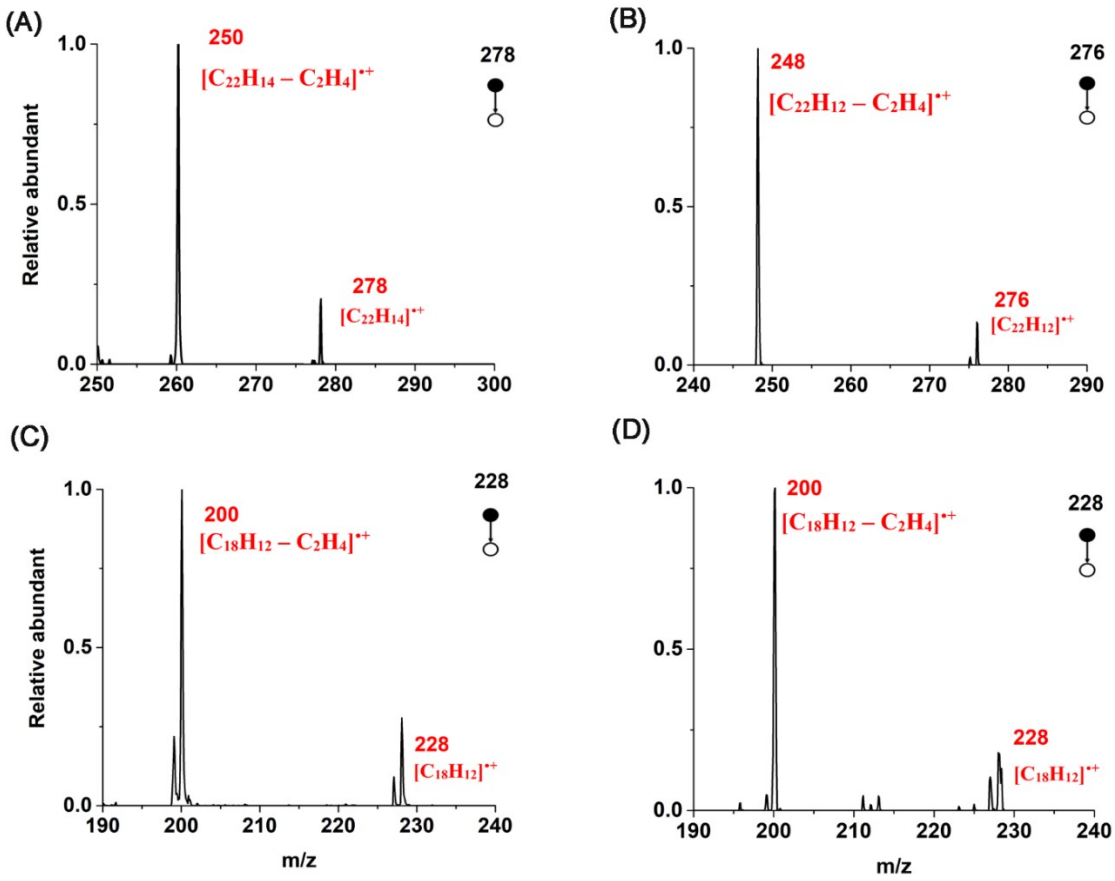

Figure S9. The CID fragmentation patterns of $M^{\bullet+}$ of different PAHs in complex biosamples: (A) $[C_{22}H_{14}]^{\bullet+}$, (B) $[C_{22}H_{12}]^{\bullet+}$ and (C) $[C_{18}H_{12}]^{\bullet+}$ in fetal bovine serum, as well as (D) $[C_{18}H_{12}]^{\bullet+}$ in a single-cell sample.

Collision-induced dissociation (CID) was used to confirm the detection of target PAHs in Figure 6 and 7. The detection result was shown in Figure S9 and Table S1. A mass loss of 28 Da was observed on all three ion species, which was supposed to be attributed to the loss of C_2H_4 during CID fragmentation. This was the typical fragmentation pattern of PAHs in CID. The result shown in Figure S9(A−C) demonstrated that the signals detected at m/z 278, 276 and 228 in Figure 6 were derived from dibenzo[a,h]anthrathracene, indeno[1,2,3-cd] pyrene and benzo[a]anthracene, respectively, in fetal bovine serum (FBS). Similarly, the results shown in Figure S9(D) confirmed that the signal at m/z 228 detected in Figure 7 originated from benzo[a]anthracene in single-cell samples.

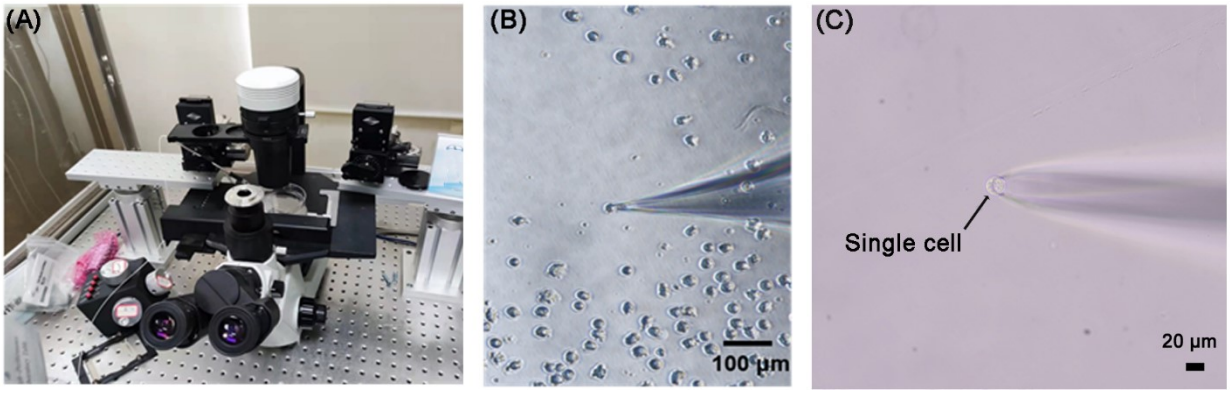

Figure S10. Images of the sampling process of single K562 cells: (A) the device image of the single-cell capturing system; (B) the microscopic image depicting the successful capture of a single K562 cell; (C) the magnified image of the capture of a single cell.

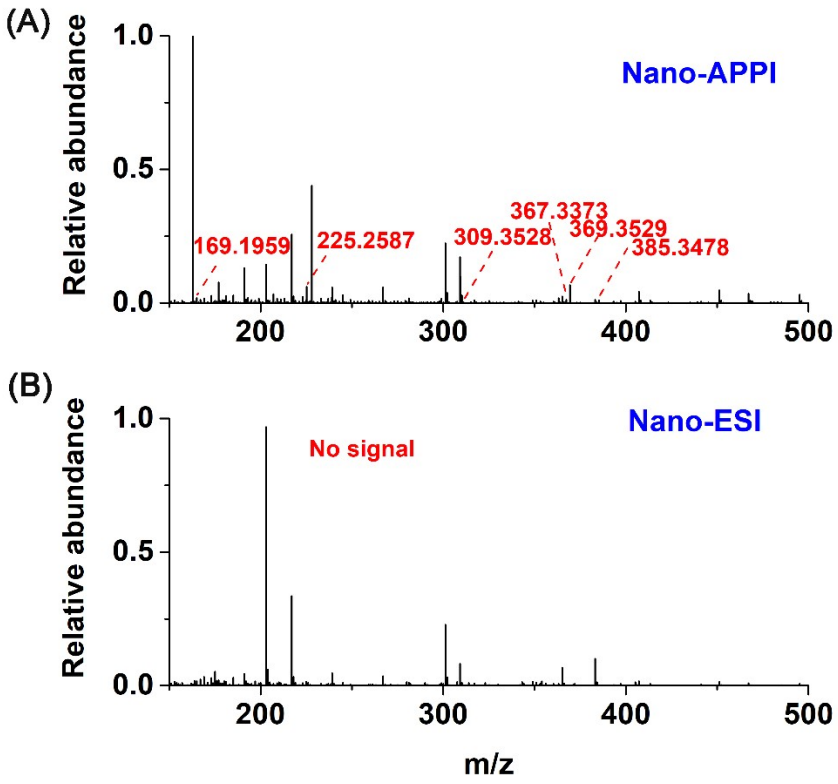

Figure S11. The successful detection of endogenous metabolites in single cells based on (A) nano-APPI and (B) nano-ESI.

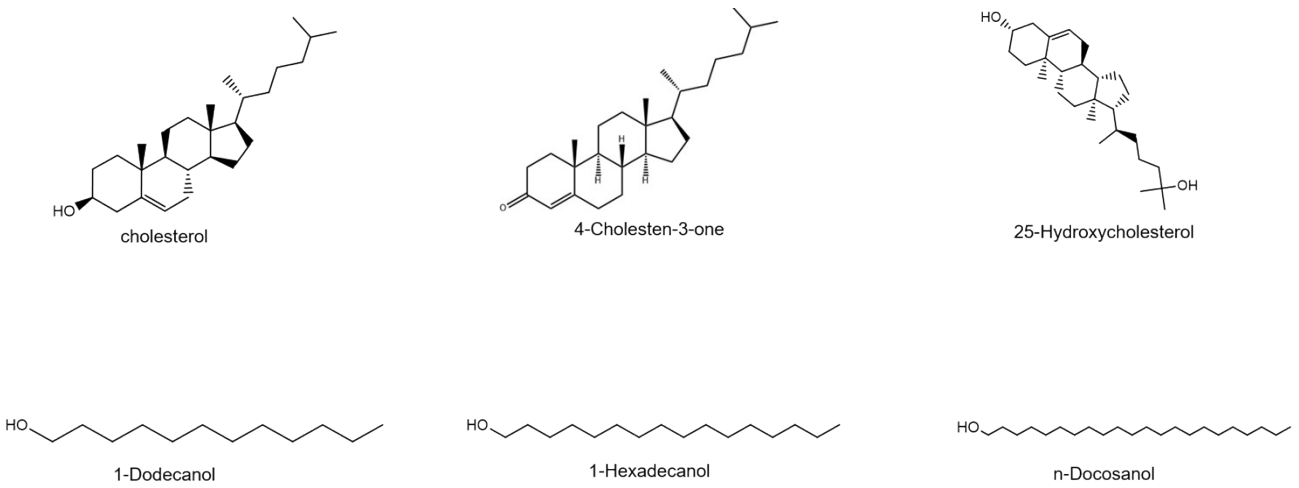

Figure S12. Chemical structure of detected sterols and fatty alcohol metabolites in single K562 cells.

Previous studies have demonstrated that sterols and fatty alcohols hold important positions in many physiological pathways and play significant roles in cellular metabolic activities.[1, 2] Nano-APPI was further used for the detection of endogenous fatty alcohols and sterols in single K562 cells. High resolution mass spectrometry (HRMS) was used for the identification of the detected endogenous substances (Figure S11 and Table S5). An Orbitrap Elite Mass Spectrometer (Thermo Scientific, San Jose, CA) was used for the detection. The resolution was set at 240 000. Three fatty alcohols and three sterols were identified in the mass spectra obtained from single K562 Cells (Figure S12). The accurate mass of the detected fatty alcohols and sterols was shown in Table S5. Except for 4-cholesten-3-one, all the other molecules were detected as dehydrated protonated ions due to the existence of intramolecular hydroxyl groups. 25-Hydroxycholesterol lost two H_2O after ionization, as it has two intramolecular hydroxyl groups. However, 4-Cholesten-3-one was detected as protonated ions, due to the fact that it has no intramolecular hydroxyl group. The results above confirmed the capacity of nano-APPI for the analysis of not only PAHs but also other endogenous metabolites. In comparison, endogenous fatty alcohols and sterols in single K562 cells cannot be detected in nano-ESI. The successful analysis of endogenous metabolites by nano-APPI in single cells might potentially be beneficial to other bioanalytical scenarios like clinical diagnosis and treatment in the future.

Table S1. The detailed information of the CID fragmentation of different PAHs ions

Compound	Parent(m/z)	Daughter(m/z)	Isolation width	Collison energy (eV)
Dibenzo[a,h]anthrathracene	278	250	1	45
Indeno[1,2,3-cd] pyrene	276	248	1	42
Benzo[a]anthracene	228	200	1	40

Table S2. List of detected PAHs in fetal bovine serum and single cells

Compound names	Sample form	Formula	Ion form	Measured m/z	Theoretical m/z	Δ_m (ppm)
Dibenzo[a,h]anthrathracene	FBS	$C_{22}H_{14}$	$[C_{22}H_{14}]^{\bullet+}$	278.1103	278.1096	−2.16
Indeno[1,2,3-cd] pyrene	FBS	$C_{22}H_{12}$	$[C_{22}H_{12}]^{\bullet+}$	276.0946	276.0939	−2.53
Benzo[a]anthracene	FBS	$C_{18}H_{12}$	$[C_{18}H_{12}]^{\bullet+}$	228.0945	228.0939	−2.63
Benzo[a]anthracene	Single-cell	$C_{18}H_{12}$	$[C_{18}H_{12}]^{\bullet+}$	228.0945	228.0939	−2.63

High resolution mass spectrometry (HRMS) was used to measure the accurate mass of $M^{\bullet+}$ peaks of different PAHs. The high resolution data was shown in Table S2. An Orbitrap Elite Mass Spectrometer (Thermo Scientific, San Jose, CA) was used. The resolution was set at 240 000. According to the results, the accurate masses of the $M^{\bullet+}$ peak measured in the mass spectrum of dibenzo[a,h]anthrathracene, indeno[1,2,3-cd] pyrene and benzo[a]anthracene in FBS were 278.1103, 276.0946 and 228.0945, respectively. The theoretical masses of dibenzo[a,h]anthrathracene, indeno[1,2,3-cd] pyrene and benzo[a]anthracene were 278.1096, 276.0939 and 228.0939, respectively. Δ_m was below 5 ppm, so we consider the successful detection of dibenzo[a,h]anthrathracene, indeno[1,2,3-cd] pyrene and benzo[a]anthracene in FBS via nano-APPI.

Similar results were obtained on benzo[a]anthracene in a single-cell sample. According to the results, the accurate mass of the $M^{\bullet+}$ peak measured in the mass spectrum of benzo[a]anthracene in a single cell was 228.0945 (Table S2). The theoretical mass of benzo[a]anthracene was 228.0939 (Table S2). Two value was the same, so we consider the successful detection of benzo[a]anthracene in a single cell via nano-APPI.

Table S3. List of detected sterol and fatty alcohol metabolites in single K562 cells

Compound names	Formula	Ion form	Measured m/z	Theoretical m/z	Δ_m (ppm)
Cholesterol	$C_{27}H_{46}O$	$[M + H - H_2O]^+$	369.3529	369.3521	−2.16
4-Cholesten-3-one	$C_{27}H_{44}O$	$[M + H]^+$	385.3478	385.3470	−2.07
25-Hydroxycholesterol	$C_{27}H_{46}O_2$	$[M + H - 2H_2O]^+$	367.3373	367.3365	−2.17
1-Dodecanol	$C_{12}H_{26}O$	$[M + H - H_2O]^+$	169.1959	169.1956	−1.77
1-Hexadecanol	$C_{16}H_{34}O$	$[M + H - H_2O]^+$	225.2587	225.2582	−2.21
n-Docosanol	$C_{22}H_{46}O$	$[M + H - H_2O]^+$	309.3528	309.3521	−2.26

Table S4. The quantification results of PAHs obtained by APCI; Benzo[a]anthracene-d_{12} was used as the internal standard (IS) with a concentration of 20 μM.

Analyte	Linear range (μM)	Calibration curve	Correlation coefficient (R)	Recovery (% RSD, n = 3)			Sensitivity	
				10 μM	100 μM	1000 μM	LOD (μM)	LOQ (μM)
Fluoranthene	0.7−1000	Y = 0.0907X – 0.1115	0.9991	83.2	90.1	98.4	0.2	0.7
Pyrene	0.8−1000	Y = 0.0877X – 0.1935	0.9972	84.7	88.5	96.7	0.3	0.8
Benzo[a]anthracene	1.2−1200	Y = 0.0511X – 0.0216	0.9986	77.3	80.0	84.3	0.4	1.2
Chrysene	1.2−1200	Y = 0.0521X – 0.0242	0.9984	80.9	83.7	89.9	0.4	1.2
Benzo[k]fluoranthene	1.4−1400	Y = 0.0325X + 0.0635	0.9989	89.7	92.8	93.5	0.5	1.4
Benzo[b]fluoranthene	1.4−1400	Y = 0.0337X + 0.0261	0.9950	82.5	85.4	94.7	0.5	1.4
Benzo[a]fluoranthene	1.4−1400	Y = 0.0308X + 0.0895	0.9979	81.5	84.6	89.9	0.5	1.4
Indeno[1,2,3-cd] pyrene	1.8−2100	Y = 0.0287X – 0.0379	0.9971	77.9	85.1	89.4	0.7	1.8
Dibenzo[a,h]anthrathracene	1.8−2300	Y = 0.0267X + 0.0395	0.9972	84.8	87.8	91.3	0.8	1.8

Table S5. The information of employed PAHs detected by nano-APPI

Analyte	Molecular weight (m/z)	The detected ion form
Naphthalene	128	$M^{\bullet+}$
Anthracene	178	
Fluoranthene	202	
Pyrene	202	
Benzo[a]anthracene	228	
Chrysene	228	
Benzo[k]fluoranthene	252	
Benzo[b]fluoranthene	252	
Benzo[a]fluoranthene	252	
Indeno[1,2,3-cd] pyrene	276	
Benzo[g,h,i]perylene	276	
Dibenzo[a,h]anthrathracene	278	

References

1. Y.-Q. Cao, L. Zhang, J. Zhang and Y.-L. Guo, *Analytical Chemistry*, 2020, **92**, 8378-8385.
2. C. H. Grün and S. Besseau, *Journal of Chromatography A*, 2016, **1439**, 74-81.